On atmospheric-pressure non-equilibrium plasma jets and plasma bullets

2012 Plasma Sources Sci. Technol. 21 034005

(http://iopscience.iop.org/0963-0252/21/3/034005)

Plasma Sources Sci. Technol. **21** (2012) 034005 (17pp) doi:10.1088/0963-0252/21/3/034005

On atmospheric-pressure non-equilibrium plasma jets and plasma bullets

X Lu[1,4], **M Laroussi**[2] **and V Puech**[3]

[1] State Key Laboratory of Advanced Electromagnetic Engineering and Technology, Huazhong University of Science and Technology, Wuhan, Hubei 430074, People's Republic of China
[2] Laser & Plasma Engineering Institute, Old Dominion University, Norfolk, VA, USA
[3] Laboratoire de Physique des Gaz et des Plasmas, CNRS & Univ. Paris-Sud, Orsay, France

E-mail: luxinpei@hotmail.com

Received 12 October 2011, in final form 5 February 2012
Published 16 April 2012
Online at stacks.iop.org/PSST/21/034005

Abstract
Atmospheric-pressure non-equilibrium plasma jets (APNP-Js), which generate plasma in open space rather than in a confined discharge gap, have recently been a topic of great interest. In this paper, the development of APNP-Js will be reviewed. Firstly, the APNP-Js are grouped based on the type of gas used to ignite them and their characteristics are discussed in detail. Secondly, one of the most interesting phenomena of APNP-Js, the 'plasma bullet', is discussed and its behavior described. Thirdly, the very recent developments on the behavior of plasma jets when launched in a controlled environment and pressure are also introduced. This is followed by a discussion on the interaction between plasma jets. Finally, perspectives on APNP-J research are presented.

(Some figures may appear in colour only in the online journal)

1. Introduction

For atmospheric-pressure non-equilibrium plasmas, the electron temperature is far higher than the temperature of the heavy particles. Due to the high collision frequency between electrons and heavy particles, the electrons lose their energy in a short period. If molecular gas is present, the electrons could quickly transfer their energy to molecular rotational and vibrational states because the energy levels of the rotational and vibrational states of the molecules can be much lower than that of the electrons' excitation and ionization [1–3]. This makes it a difficult task to obtain atmospheric-pressure non-equilibrium plasmas with high electron energy. Thus, the ionization efficiency in such a case is low. Furthermore, when an electronegative gas, such as O_2 and SF_6, is present, the electrons could be absorbed by the gas on a time scale of tens of nanoseconds, or even shorter, which makes it even harder to obtain atmospheric-pressure non-equilibrium plasmas with electronegative gases [4].

Nevertheless, for traditional discharges, a plasma is generated as long as the applied electric field across the discharge gap is high enough to initiate a breakdown. However, at a pressure of 1 atm, the electric field required to initiate the discharge is quite high. For example, when air is used, the required electric field is about $30\,\mathrm{kV\,cm^{-1}}$. That is why the discharge gaps for most atmospheric-pressure discharges are from mm to several cm [5–13]. On the other hand, from the applications point of view, the short discharge gaps significantly limit the size of the objects to be treated if direct treatment (when the object is placed between the gaps) is desired. If indirect treatment (the object is placed next to the gaps and the active radicals of the plasma reach the object by flowing with the gas) is applied, active radicals with short lifetimes and charged particles may already disappear before reaching the sample to be treated. To overcome the shortcomings of the traditional atmospheric-pressure non-equilibrium plasmas, plasmas generated in open space rather than in a confined discharge gap are needed. However, when a plasma is to be launched in open space where the applied electric field is normally quite low, it is extremely difficult to sustain the existence of the plasma.

Briefly, as pointed to above, there are two facts that make it a big challenge to generate atmospheric-pressure non-equilibrium plasma jets (APNP-J), one is the high electron–heavy particle collision frequency, and the other is the low

[4] Author to whom any correspondence should be addressed.

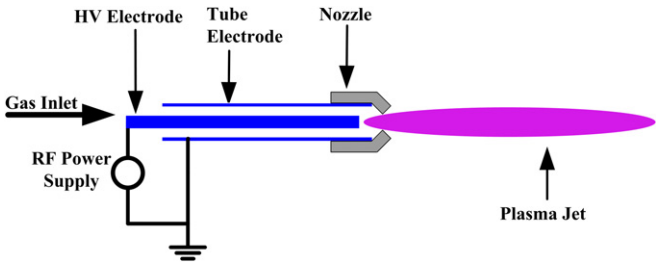

Figure 1. Schematic of a dielectric-free electrode (DFE) jet [14].

applied electric field. Fortunately, various methods were developed to overcome these challenges and several sources based on different designs were subsequently reported [14–78]. APNP-Js are generated in open space rather than in confined gaps. Thus, they can be used for direct treatment and there is no limitation on the size of the object to be treated. This is extremely important for applications such as plasma medicine [79–106]. In this paper, the development of APNP-Js will be reviewed. The paper is organized as follows: First, since the working gas is one of the main factors that affect the characteristics of APNP-Js, the APNP-Js are grouped based on the type of gas used to ignite them. Second, one of the most interesting phenomena of APNP-Js, the 'plasma bullet', is discussed and its behavior is described. This is followed by a section devoted to a presentation of very recent developments on the behavior of plasma jets when launched in a controlled environment and pressure. Finally, the interaction between plasma jets is discussed in the last section.

2. Plasma jets

2.1. Noble gas plasma jet

Various types of APNP-Js with different configurations have been reported, where most of the jets are working with noble gas mixed with a small percentage of reactive gases, such as O_2. Plasma jets operating with noble gases can be classified into four categories, i.e. dielectric-free electrode (DFE) jets, dielectric barrier discharge (DBD) jets, DBD-like jets and single electrode (SE) jets, as shown in figures 1–4.

2.1.1. DFE jets. One of the early APNP-Js, developed by Hicks' group, is a DFE jet, as shown in figure 1 [14, 15]. The jet is driven by a radio frequency (RF) power source at 13.56 MHz. It consists of an inner electrode, which is coupled to the power source, and a grounded outer electrode. A mixture of He with reactive gases is fed into the annular space between the two electrodes. Cooling water is needed to keep the jet from overheating and the gas temperature of the plasma jet varies from 50 to 300 °C, depending on the RF power. The window of stable operation without apparent arcing of the device uses He flow rates greater than 25 l min^{-1}, O_2concentrations of up to 3.0% by volume, CF_4 concentrations of up to 4.0% by volume, and RF power between 50 and 500 W.

Several notable characteristics of the DFE jet are, firstly, that arcing is unavoidable when the stable operation conditions are not met. Secondly, compared with DBD and DBD-like jets (discussed below), the power delivered to the plasma for the DF jet is much higher. Thirdly, due to the high power delivered, the gas temperature of the plasma is quite high and out of the acceptable range for biomedical applications. Fourthly, for this DFE jet, which is driven by an RF power supply, the peak voltage is only a few hundred volts, so the electric field within the discharge gap is relatively low and its direction is radial (perpendicular to the gas flow direction). The electric field in the plasma plume region is even lower, especially along the plasma plume propagation direction (gas flow direction). Finally, since the electric field along the plasma plume propagation direction is very low, the generation of this plasma plume is probably gas flow driven rather than electrically driven.

On the other hand, because a relatively high power can be delivered to the plasma and the gas temperature is relatively high, the plasma is very reactive. This kind of plasma jet is suitable for applications such as material treatment as long as the material to be treated is not very sensitive to high temperatures.

2.1.2. DBD jets. For DBD jets, as shown in figures 2(*a*)–(*e*), there are many different configurations. As shown in figure 2(*a*), which was first reported by Teschke *et al* [25], the jet consists of a dielectric tube with two metal ring electrodes on the outer side of the tube. When a working gas (He, Ar) flows through the dielectric tube and kHz high-voltage (HV) power supply is turned on, a cold plasma jet is generated in the surrounding air. The plasma jet only consumes a power of several watts. The gas temperature of the plasma is close to room temperature. The gas flow velocity is less than 20 m s^{-1}. The plasma jet, which looks homogeneous to the naked eye, is actually a 'bullet'-like plasma volume with a propagation speed of more than 10 km s^{-1}. It is believed that the applied electric field plays an important role in the propagation of the plasma bullet. More discussion on this phenomenon will be given in section 3.

Figure 2(*b*) eliminates one ring electrode [26], so the discharge inside the dielectric tube is weakened. Figure 2(*c*) replaces the HV ring electrode with a centered pin electrode, which is covered by a dielectric tube with one end closed [27]. With this configuration, the electric field along the plasma plume is enhanced. Walsh and Kong's studies show that a high electric field along the plasma plume is favorable for generating long plasma plumes and more active plasma chemistry [28]. Figure 2(*d*) further removes the ground ring electrode of figure 2(*b*) [29], so the discharge inside the tube is also weakened. On the other hand, a stronger discharge inside the discharge tube (as in the case of figures 2(*a*) and (*c*)) helps the generation of more reactive species. With the gas flow, the reactive species with relatively long lifetimes may also play an important role in various applications. The configuration of figure 2(*e*), developed by Laroussi and Lu [30], is different from the previous four DBD jet devices. The two ring electrodes are attached to the surface of two centrally perforated dielectric disks. The holes in the center of the disks are about 3 mm in diameter. The distance between

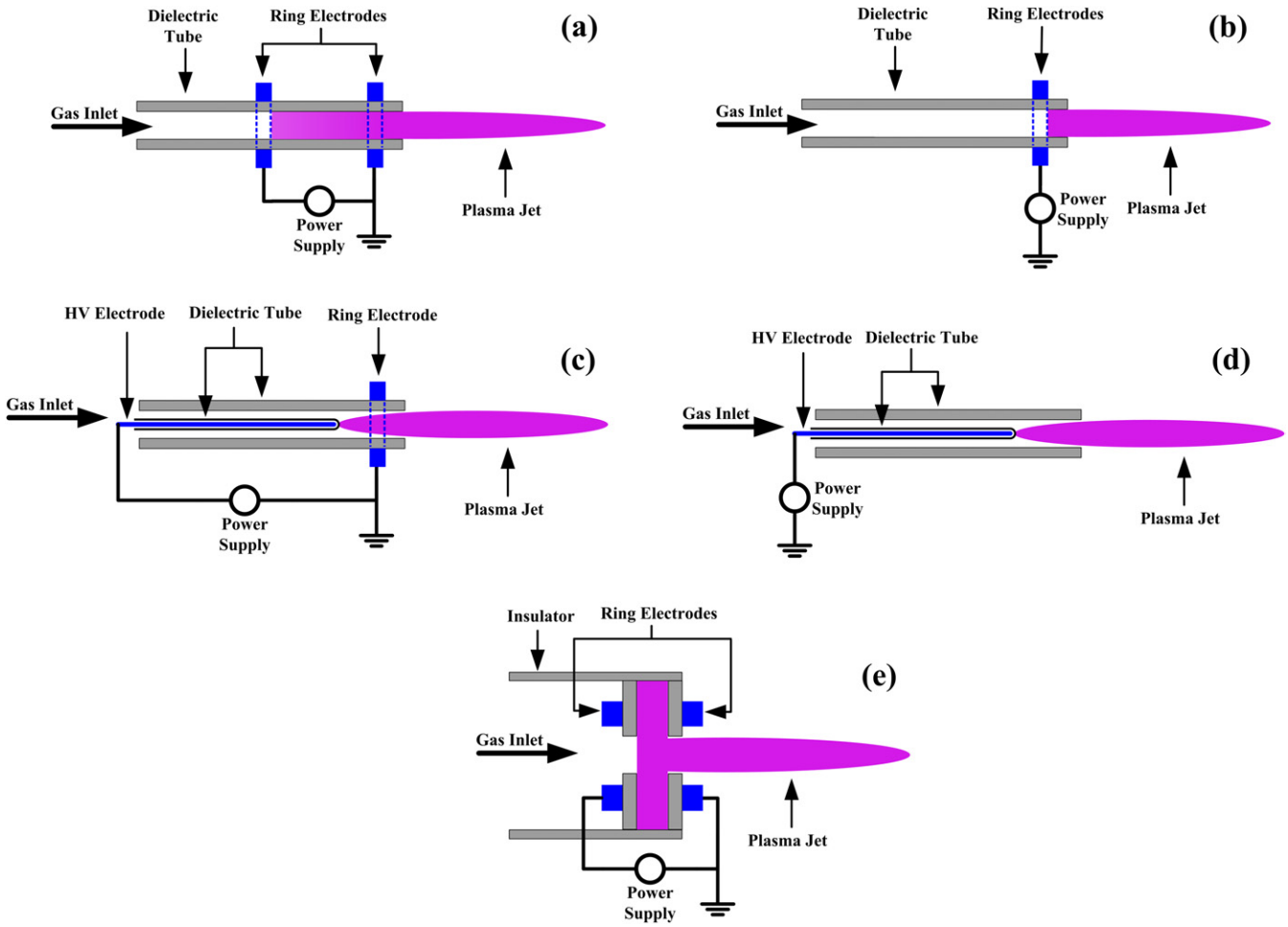

Figure 2. Schematic of a DBD plasma jet.

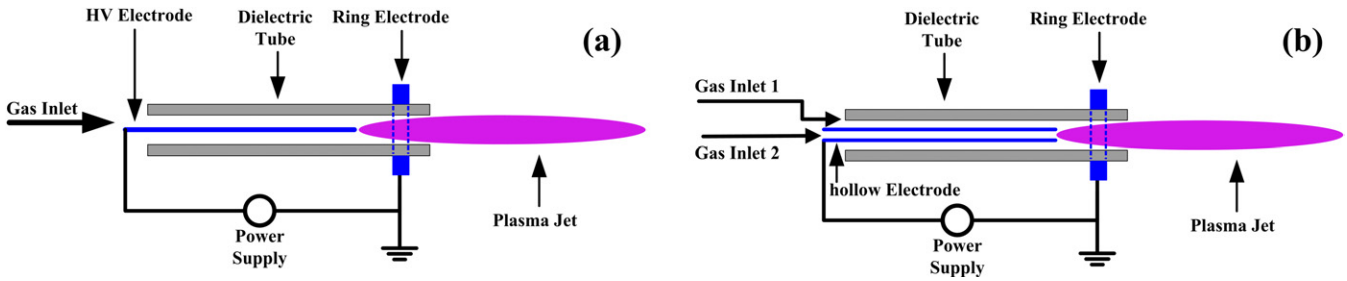

Figure 3. Schematic of a DBD-like plasma jet.

the two dielectric disks is about 5 mm. With this device, a plasma plume of up to several centimeters in length can be obtained.

All the DBD jet devices discussed above can be operated either by kHz ac power or by pulsed dc power. The length of the plasma jet can easily reach several centimeters or even longer than 10 cm, as reported by Lu *et al* [27]. This capability makes the operation of these plasma jets easy and practical. There are several other advantages of the DBD jets. Firstly, due to the low power density delivered to the plasma, the gas temperature of the plasma remains close to room temperature. Secondly, because of the use of the dielectric, there is no risk of arcing whether the object to be treated is placed far away or close to the nozzle. These two characteristics are very important for applications such as plasma medicine, where safety is a strict requirement.

2.1.3. DBD-like jets. All the plasma jet devices shown in figure 3 are named DBD-like jets. This is based on the following facts. When the plasma plume is not in contact with any object, the discharge is more or less like a DBD. However, when the plasma plume is in contact with an electrically conducting (a non-dielectric material) object, especially a ground conductor, the discharge is actually running between the HV electrode and the object to be treated (ground conductor). For such a circumstance, it no longer

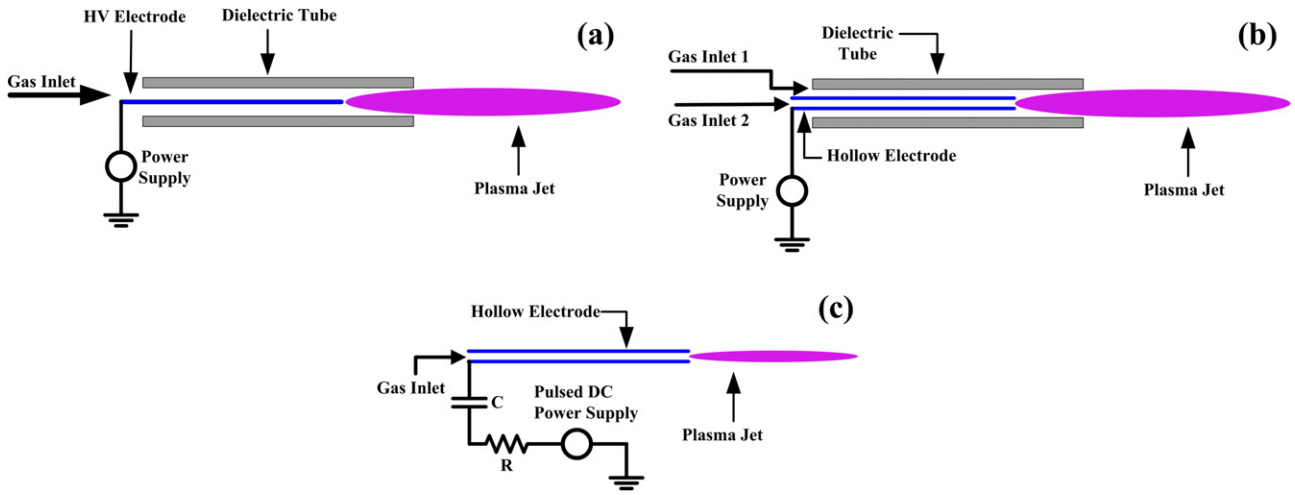

Figure 4. Schematic of an SE plasma jet.

operates as a DBD. The devices shown in figure 3 can be driven by kHz ac power, by RF power or by pulsed dc power.

Figure 3(*b*) replaces the solid HV electrode in figure 3(*a*) with a hollow electrode [22, 31]. The benefit of this kind of configuration is that two different gases can be mixed in the device. Normally, gas inlet 2 is used for a reactive gas such as O_2 flow, and gas inlet 1 is for a noble gas. It was found that the plasma plume is much longer with this kind of gas control than that using a pre-mix gas mixture with the same percentage [22]. The role (and advantage) of the ring electrode in figures 3(*a*) and (*b*) is the same as in the case of DBD jets.

When the DBD-like plasma jets are used for plasma medicine applications, the object to be treated could be cells or whole tissue. In this case, these types of jet devices should be used carefully because of the risk of arcing. On the other hand, if it is used for treatment of conductive materials, since there is no dielectric, more power can easily be delivered to the plasma. So as long as arcing is carefully avoided, the DBD-like jets have their own advantages.

2.1.4. Single electrode (SE) jets. The schematics of single electrode (SE) jets are shown in figures 4(*a*)–(*c*). Figures 4(*a*) and (*b*) are similar to the DBD-like jets except there is no ring electrode on the outside of the dielectric tube. The dielectric tube only plays the role of guiding the gas flow. These two jets can be driven by dc, kHz ac, RF or pulsed dc power.

Because of the risk of arcing, the plasma plumes generated by figures 4(*a*) and (*b*) are not the best for biomedical applications due to safety issues [32]. In order to overcome this problem, Lu *et al* developed a similar SE jet, as shown in figure 4(*c*) [33]. The capacitance C and resistance R are about 50 pF and 60 kΩ, respectively. The resistor and capacitor are used for controlling the discharge current and voltage on the hollow electrode (needle). This jet is driven by a pulsed dc power supply with a pulse width of 500 ns, repetition frequency of 10 kHz and amplitude of 8 kV. The advantage of this jet is that the plasma plume or even the hollow electrode can be touched without any risk of injury, making it suitable for plasma medicine applications.

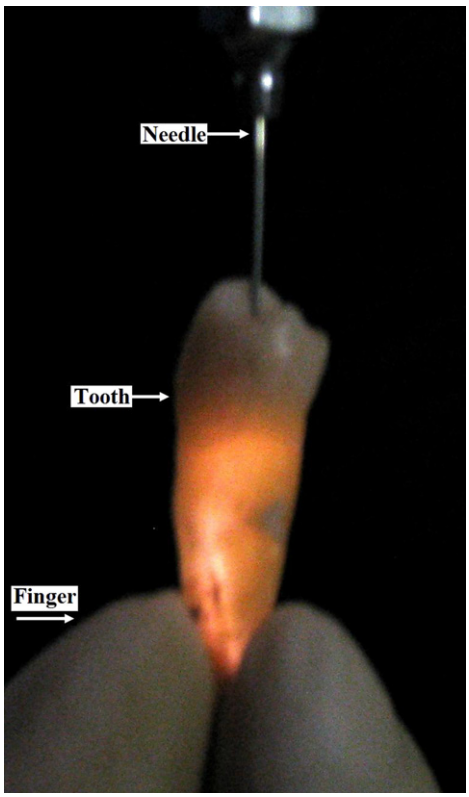

Figure 5. Photograph of a plasma generated in the root canal of a tooth using the jet of figure 4(*c*) [33].

One of the potential applications is in dentistry, such as root canal treatment. Due to the narrow channel geometry of a root canal, which typically has a length of few centimeters and a diameter of one millimeter or less, the plasma generated by a plasma jet is not efficient to deliver reactive agents into the root canal for disinfection. Therefore, to have a better killing efficacy, a plasma needs to be generated inside the root canal, whereupon reactive agents, including the short-lifetime species, such as charged particles, could play some role in the killing of bacteria. Using the device of figure 4(*c*), a cold plasma could be generated inside a root canal, as shown in figure 5.

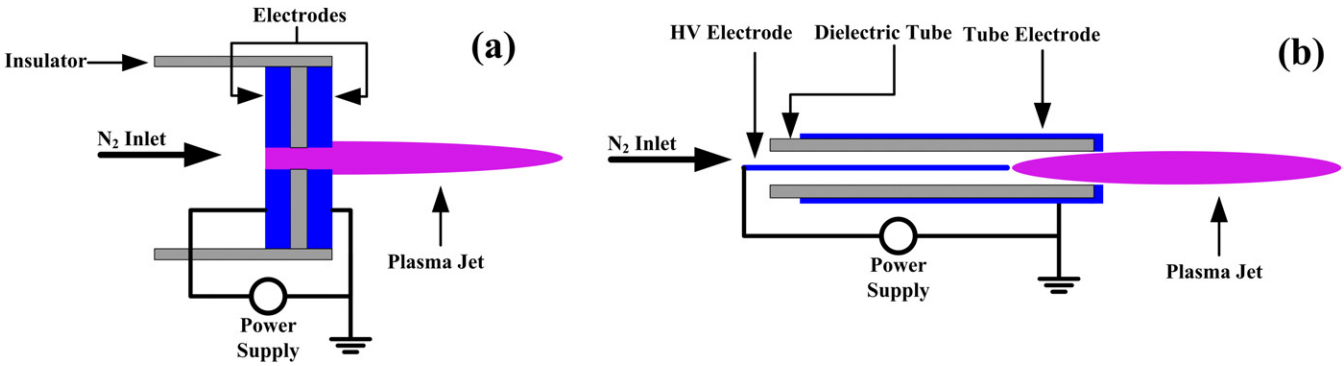

Figure 6. Schematic of a N_2 plasma jet.

2.2. N_2 plasma jet

As pointed out in section 1, it is difficult to generate atmospheric-pressure non-equilibrium nitrogen (N_2) plasma jets. Up to now, only a few N_2 plasma jets have been reported [34–36]. Figure 6 shows the schematic of two N_2 plasma jets. The N_2 plasma jet as shown in figure 6(*a*) was reported by Hong and Uhm [34]. A 20 kHz ac power supply is connected to two electrodes of thickness 3 mm and a center hole of diameter 500 μm. The two electrodes are separated by a dielectric disk with a center hole of the same diameter. With this configuration, they are capable of generating a N_2 plasma up to 6.5 cm long. When the N_2 gas flow rate is 6.3 slm (standard liters per minute), the gas is ejected out from the hole at a speed of about 535 m s^{-1}. The gas temperature of the plasma plume at 2 cm from the nozzle is below 300 K. Figure 6(*b*) shows a slightly different N_2 plasma jet device, which replaces the inner perforated HV electrode of figure 6(*a*) by a pin electrode [35]. The inner electrode can also be replaced by a tube such as the one used by Hong *et al* [36].

2.3. Air plasma jet

Due to the presence of electronegative oxygen, O_2, in air it is difficult to sustain an atmospheric-pressure non-equilibrium air plasma jet. Nevertheless, several different air plasma jets have been reported [37–41]. Mohamed *et al* reported a micro-plasma jet device that can operate in various gases including air [38]. The schematic is shown in figure 7(*a*). A discharge channel through an insulator with a thickness of about 0.2–0.5 mm and a diameter of 0.2–0.8 mm separates the anode and the cathode, which have a center hole of the same diameter. The ballast resistor is 51 kΩ. When air flows through the hole and a dc voltage of a few hundred volts (up to a kV) is applied between the anode and cathode (depending on the thickness of the insulator separating the electrodes), a relatively low temperature air plasma is generated in the surrounding air with length up to 1 cm, depending on the gas flow rate and discharge current. However, the gas temperature of the plasma can still be quite high. The gas temperature within the micro-gap is about 1000 K. However, it drops quickly as it propagates in the surrounding air. It is about 50 °C at 5 mm away from the nozzle for an air flow rate of 200 ml min^{-1} and discharge current of 19 mA.

Hong *et al* reported another type of air plasma jet device as shown in figure 7(*b*) [39]. One of the notable characters of this device is that a porous alumina dielectric is used to separate the HV stainless steel (typical injection needle) electrode and the outer ground electrode. The alumina used in this device has approximately 30 vol% porosity and has an average pore diameter of 100 μm. The ground electrode is fabricated from stainless steel and has a centrally perforated hole of 1 mm diameter through which the plasma jet is ejected to the surrounding ambient air. When 60 Hz HV power supply is applied and the flow rate of air is at several slm, an APNP-J up to about 2 cm is generated in the surrounding air. During one voltage cycle, there are multiple discharges. The increase in the input power results in more current pulses. The shortcoming of this device is the same as the previous one, i.e. the gas temperature of the plasma is quite high. It is about 60 °C at 10 mm away from the nozzle for an air flow rate of 5 slm. For lower flow rates, the gas temperature is even higher.

Figures 7(*c*) and (*d*) are the schematics of two 'floating' electrode air plasma jets [40, 41]. Strictly, they are not plasma jets since the plasmas are generated within a gap. However, because the secondary electrode (ground electrode) can be a human body, so we still categorize them as plasma jets in this paper. Both jets could generate room temperature air plasmas. They are completely safe from the electrical perspective and non-damaging to animals or human beings.

For figure 7(*c*), kHz ac or pulsed dc voltage with an amplitude of 10–30 kV is used to drive the device. The discharge ignites when the powered electrode approaches the surface to be treated at a distance (discharge gap) of less than about 3 mm, depending on the form, duration and polarity of the driving voltage. This jet is suitable for large smooth surface treatment.

In contrast, the jet shown in figure 7(*d*) is more suitable for localized three-dimensional treatments. This jet is driven by a homemade dc power supply. The output voltage of the power supply can be adjusted up to 20 kV. The output of the power supply is connected to a stainless steel needle (typical injection needle) electrode through a resistor R of 120 MΩ, which is several orders of magnitude higher than those reported [42]. When a counter-electrode, such as a finger, is placed close to the needle, a plasma is generated, as shown in figure 8. The plasma is similar to the positive corona discharge. However,

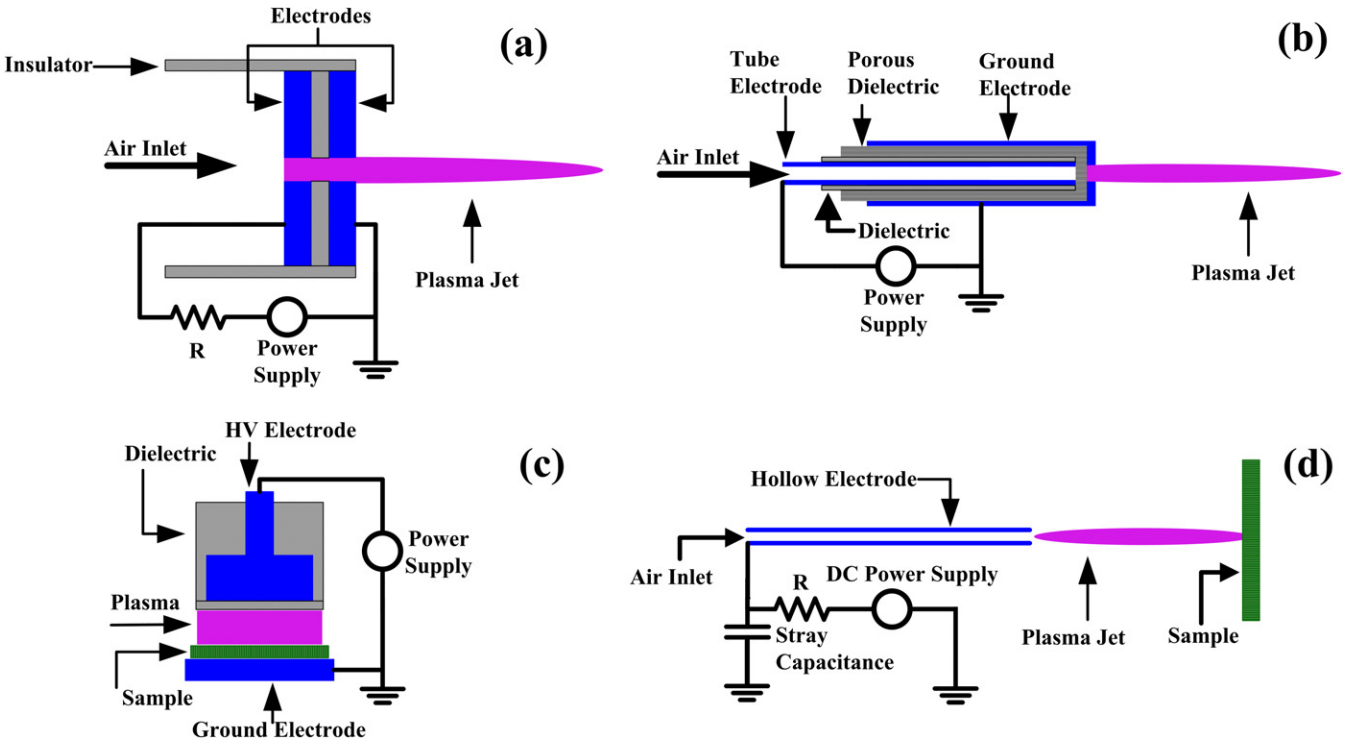

Figure 7. Schematic of an air plasma jet.

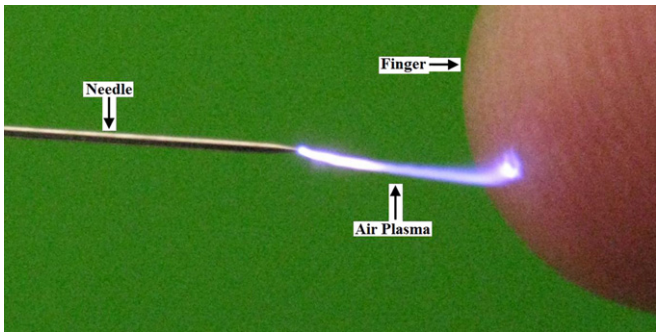

Figure 8. Plasma generated by a dc power supply touched by a finger [41].

this jet can be touched by the human body directly, which is not the case for the traditional corona discharge. The jet has no risk of glow–arc transition. The maximum length of the plasma is about 2 cm. The gas temperature of the plasma is kept at room temperature. It is interesting to point out that the discharge is actually pulsed. It appears periodically with a pulse frequency of tens of kHz, depending on the applied voltage and distance between the tip of the needle and the object to be treated, as shown in figure 9.

It should be pointed out that all these air plasma jets can also be operated with N_2 gas. On the other hand, the device shown in figure 6(*a*) can be operated with air too. But the maximum length of the air plasma plume operated with the jet shown in figure 6(*a*) is about 2 cm. In addition, the jet shown in figure 4(*c*) can be operated with air as a working gas [43]. But the length of the plasma is only several millimeters.

2.4. Brief summary

Although noble gas plasma jets are relatively easy to generate, they are not as reactive as air plasma jets. That is the reason why a small percentage of reactive gases are added to the noble gas when the plasma jets are used for various applications. The noble gas is used to serve as the carrier gas to generate the plasma. For biomedical applications, O_2 or H_2O_2 is usually added. For applications of etching, CF_4 or O_2 could be used. Regarding N_2 plasma jets, they are also not as reactive as air plasma jets. It is also recommended to add a small percentage of reactive gases to the carrier gas.

3. Plasma bullet

The discrete nature of the structure of plasma jets was first observed by Teschke *et al* using an RF-driven plasma jet [25] and by Lu and Laroussi using a pulsed dc plasma jet (the plasma pencil) [109]. Using fast imaging, these investigators found that the plasma plume, which appeared continuous to the naked eye, was in fact made up of fast moving plasma structures. Teschke *et al* found that the small volume of plasma, or plasma bullet, travels at a velocity of about 1.5×10^4 m s^{-1} [25] while Lu and Laroussi measured velocities as high as 1.5×10^5 m s^{-1} [109]. Comparatively, the estimated upper limit of the drift velocity of electrons under the external applied electric field is only 1.1×10^4 m s^{-1}, and the estimated upper limit of theN_2^+ drift velocity is 2.2×10^2 m s^{-1}. Because these speeds are far lower than the measured bullet-like plume velocity, Lu and Laroussi invoked a streamer propagation model based on photoionization, in the manner that was proposed by Dawson

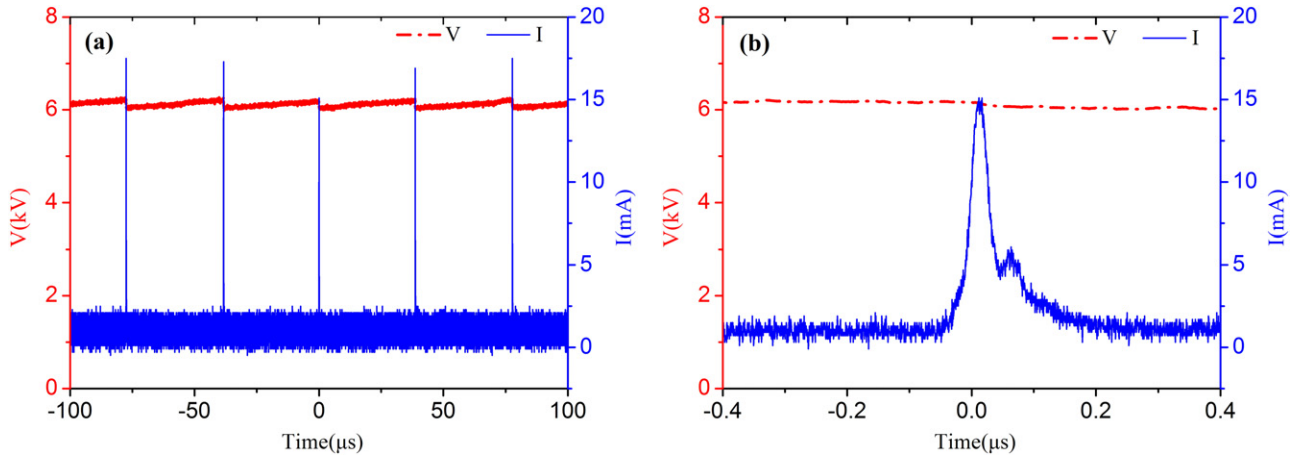

Figure 9. (*a*) Typical I–V characteristics of the plasma and (*b*) a close look on the I–V characteristics of a typical single pulse [41].

and Winn [110] for streamers, to explain the properties of these so-called plasma bullets.

However, there are some notable differences between the streamer-like APNP-J and positive corona discharges that are typically used to study cathode-directed streamers. For example, streamers developed in pulsed positive corona discharges are typically not very repeatable due to the stochastic nature of their initiation. In contrast, the plasma bullet behavior is mostly very repeatable. In addition, experiments revealed ring-shaped profiles of plasma bullet radiation, of the densities of nitrogen ions and metastable He atoms, with maxima shifted from the jet axis. Such a pattern is different from that of a typical streamer in uniform media, which does not have a donut-shaped structure. In addition, the propagation of the plasma plume left a dark channel between the plume head and the electrode. It is not clear yet whether the conductivity of the dark channel is high enough to affect the propagation of the plasma plume as in a streamer discharge or not. Furthermore, photoionization plays an important role in positive streamers. However, it is not clear whether photoionization plays a similar role in the propagation of the plasma bullet either. Finally, in a streamer discharge, the discharge behaves differently when the polarity of the voltage is changed from positive to negative. How plasma jets behave for different polarities also needs investigation. Because of the vast difference between streamers and the bullet-like plasma plume, many studies have been carried out to investigate the so-called 'plasma bullet' behavior in recent years [69, 111–146]. Some of these questions are now much better understood. In the next section, recent studies pertaining to these issues will be discussed.

3.1. Stochastic or repeatable characteristics of plasma bullets

It was believed that plasma plume propagation behaves in a repeatable fashion: they consistently propagate the same distance after the same propagation time. Xian *et al* found that under certain conditions this may not be the case. The jet used by Xian *et al* is similar to that shown in figure 4(*c*) [109]. When a pulsed dc voltage is applied, as shown in figure 10, the discharge exhibits a chaotic mode when the applied voltage is 8 kV. On the other hand, when the applied voltage is increased to 9 kV, the discharge becomes repeatable.

The set-up used by Walsh *et al* is similar to figure 2(*b*) except that they put a ground electrode in front of the plasma jet [112]. Through detailed electrical and optical characterization, Walsh *et al* also found that immediately following breakdown the plasma jet operates in a chaotic mode. By increasing the applied voltage, the discharge becomes periodic and the jet plasma is found to produce at least one strong plasma bullet for every cycle of the applied voltage. These results show that under certain conditions plasma plumes can also exhibit a stochastic behavior.

3.2. 'Donut' shape of the plasma bullet

Teschke *et al* and Mericam-Bourdet *et al* observed that the plasma bullet is, in fact, hollow and has a 'donut', or ring-shaped, structure, as shown in figure 11 [25, 113].

These observations have subsequently been supported by Sakiyama *et al* and Naidis through computer simulation [114, 115]. Naidis showed that for a helium jet propagating in air, the propagation is mainly due to confinement of the discharge front in the channel, where the air molar fraction x is less than 0.01, as the direct ionization rate in helium–air mixtures decreases sharply for higher values of x [115]. Naidis showed that the discharge has a ring shape as it propagates at the interface where $x = 0.01$ [115].

Figure 12 shows the radial profiles of the number densities of electrons n_e and $N_2(C\,^3\Pi)$ molecules $n_{N_2(C)}$ at axial positions $z = 1, 2$ and 4 cm, just after the arrival of the streamer front. It clearly shows that the maxima of n_e and $N_2(C\,^3\Pi)$ are shifted from the axis to some distance, which decreases with an increase in z. The distance nearly corresponds to the position where the air molar fraction is equal to 10^{-2} [115]. The figures also show that the Penning process does have a quantitative effect on streamer parameters, though the patterns of streamer structure in both cases, with and without the Penning process, are nearly the same. This is consistent with the experimental observation by Zhu *et al* [116].

Since the 'donut' shape is related to the gas composition due to air diffusion, Wu *et al* added 1.5% of N_2 into the He

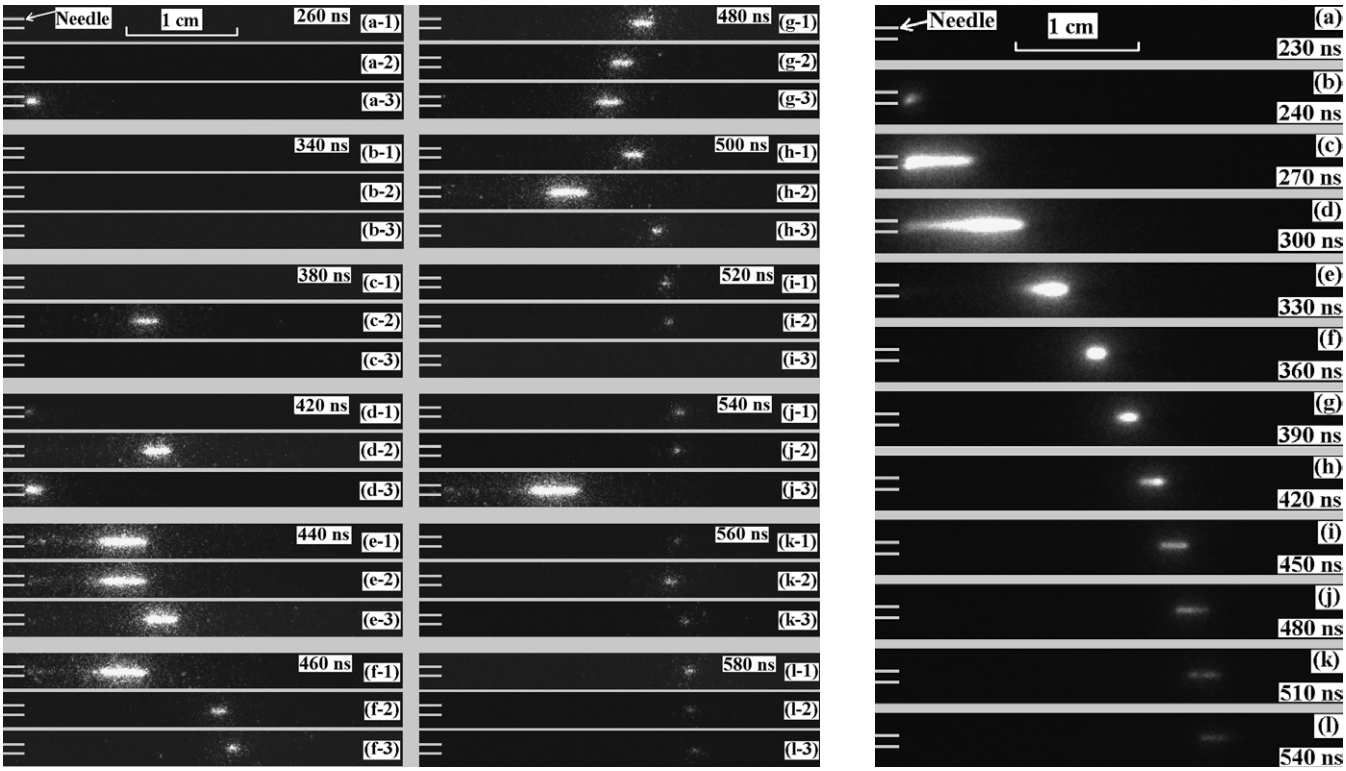

Figure 10. High-speed photographs of the plasma plume for (*a*) 8 kV and (*b*) 9 kV. For (*a*), due to the randomness of the discharges, three photographs are taken for every delay time. Pulse frequency: 10 kHz, pulsewidth: 500 ns, working gas: He/O_2 (20%), and total flow rate: 0.4 L min^{-1} [109].

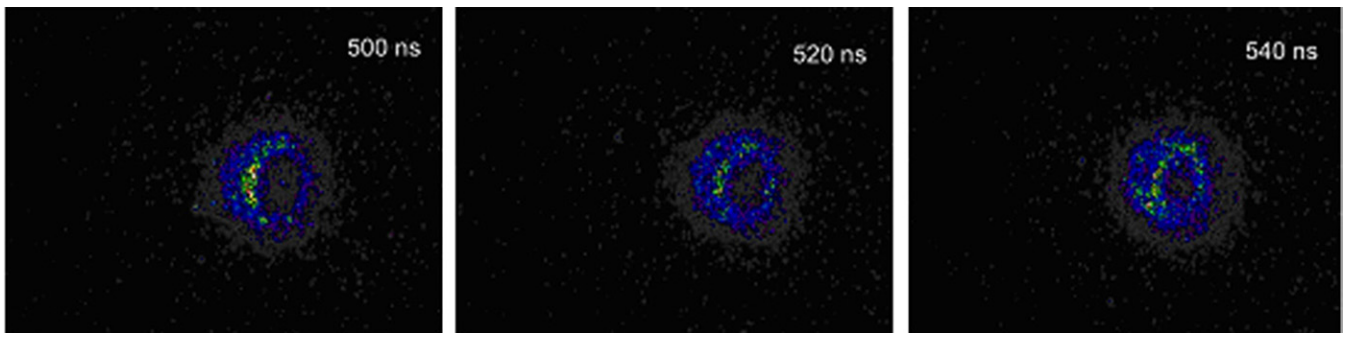

Figure 11. Photographs of bullets illustrating their donut shape [111].

gas flow and found that the 'donut' shape is replaced by a 'solid disk' shape (see figure 13). This further confirms that the 'donut' shape is due to air diffusion.

3.3. Dark channel left by the plasma bullet

It was noted that, with the propagation of the bullet-like plasma plume, a dark channel between the head of the plasma plume and the electrode exists. Lu *et al* and Karakas *et al* used the same plasma jet as shown in figure 2(*e*) to study the effect of the dark channel [118, 119]. A pulsed dc voltage was used to drive the plasma. Lu *et al* found that, as long as the pulse width is longer than 500 ns, the adjustment of the pulse width does not affect the shape and peak value of the discharge current pulses. In other words, when the pulse width is increased to more than 500 ns, it has no more of an effect on the discharge current than changing the zero current duration. Therefore, the increase in the plasma plume length with the increase in the pulse width from 500 ns to 1 μs can only be attributed to the electric field effect. Thus, although the channel left by the ionization front (plasma bullet) appears dark, based on the high-speed photographs of the plasma, the conductivity of this dark channel is not negligible; it affects the propagation of the plasma bullet. Karakas and Laroussi measured the temporal emission behavior of excited N_2, N_2^+ and He from the plasma plume at 2 cm away from the nozzle. It was found that the magnitude of the emission intensity first increases and eventually reaches its highest value. This region corresponds to the point where the ionization front propagates forward. Then, the emission decreases exponentially until it

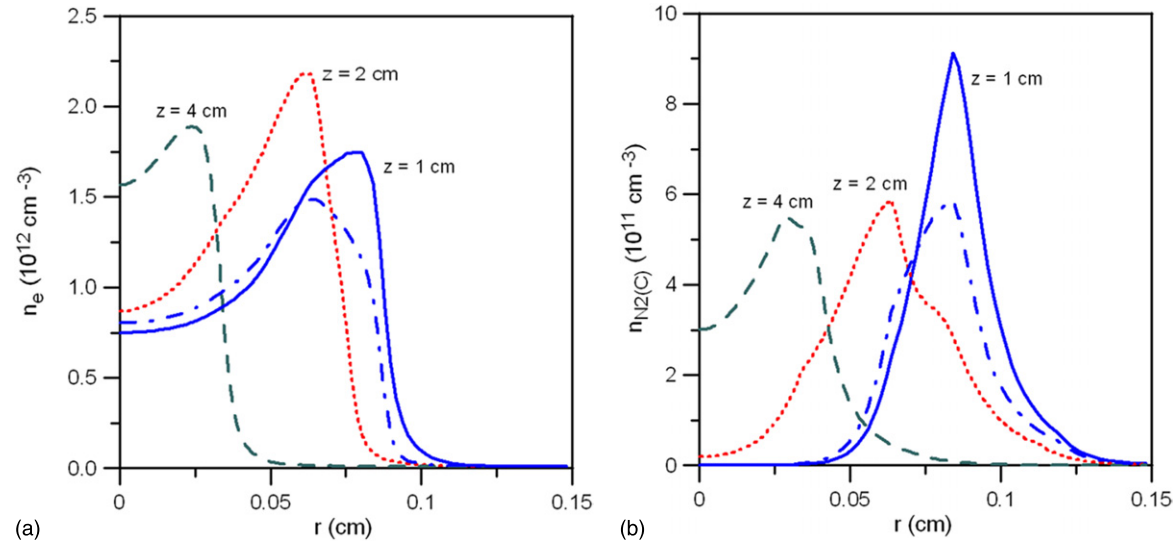

Figure 12. Radial distributions of number densities of electrons (a) and N2 ($C\,^3\Pi$) molecules (b) at various axial positions, for $z = 1$ cm, $z = 2$ cm and $z = 4$ cm. Dotted–dashed lines show the results for $z = 1$ cm obtained without taking into account the Penning reactions [115].

reaches low emission levels. The ionization front leaves behind it a channel with low concentrations of short-lived reactive species. This channel initially appears as an extension of the plasma bullet, but if the applied voltage is sufficiently high, the plasma bullet eventually breaks off this extension. Even when the plasma bullet breaks off, the secondary discharge ignition is still able to inhibit the propagation of the plasma bullet. This further confirms that the conductivity of the dark channel left by the ionization front is not negligible. Sands *et al* used a unipolar pulsed voltage to drive a jet device like the one shown in figure 2(b) [120]. They used He mixed with 5% Ar as the working gas. It was found that the Ar ($1s_5$) column density remained greater than 10^{11} cm^{-2} for up to 10 μs after the discharge was initiated, as shown in figure 14. This confirms that there are some long-lifetime species that are present in the channel and that could affect the plasma plume propagation.

Naidis simulated the distribution of the absolute value of electric field along the plasma plume [51]. He found that the maximum electric field values for the positive streamer are much higher than those for the negative one. In contrast, the electric field in the channel of a negative streamer is much higher than that in the positive one. Naidis also pointed out that, while at positive polarity, radiation is emitted mainly from a small region adjacent to the streamer head, at negative polarity the whole channel is radiating [51]. This feature is related to the difference between the electric field values in the channels of positive and negative streamers. At positive polarity the electric field in the channel is low and production of $N_2(C\,^3\Pi)$ molecules is insignificant. As the lifetime of $N_2(C\,^3\Pi)$ is much smaller than the time of streamer propagation, $N_2(C–B)$ radiation is localized in a small region near the head. At negative polarity the values of the electric field are much higher, so that $N_2(C\,^3\Pi)$ molecules are generated effectively in the whole channel [51]. In this respect, plasma jets driven by negative voltage pulses are similar to a glow plasma.

3.4. Role of photoionization

It is difficult to study the role of photoionization in the propagation of the plasma plume. In order to study the effect of photoionization, Naidis used two 2D axially symmetric positive streamer models to simulate the plasma plume [115, 121]. In one of the models, the photoionization effect was included [121] and in the other model, photoionization is neglected [115]. It is assumed instead that the streamers propagate in a uniformly weak pre-ionized gas. The initial background electron density is at a level of 10^{10} cm^{-3}. In both of the two models, the external field (the field in the absence of volume charges inside the streamers) is assumed to be constant in time and is evaluated as that produced by a positively charged sphere. The simulation results show that the streamer front moves along the jet with a mean velocity of about 10^7 cm s^{-1} based on both models. This is close to the experimental observations. Since photoionization effects could be replaced by a pre-ionization channel, so it is still not clear whether photoionization plays an essential role in the propagation of the plasma plume or not. Figure 15 shows the profiles of the electric field and the number density of electrons along the symmetry axis at various times based on the photoionization model. The line at $t = 0$ shows the external electric field and the initial electron density in figures 15(a) and (b), respectively. As can be seen, the electron density in the discharge channel reaches higher than 10^{12} cm^{-3}.

3.5. Effect of polarity of the applied voltage

Jiang *et al* and Xiong *et al* did comparative studies on the effects of the polarities of the applied voltages on the propagation of plasma plumes [122, 123]. They found that the plasma plume is much longer when positive pulsed voltages are used. In addition, the maximum velocities of the plasma plumes driven by positive voltages are higher than those driven by negative voltages.

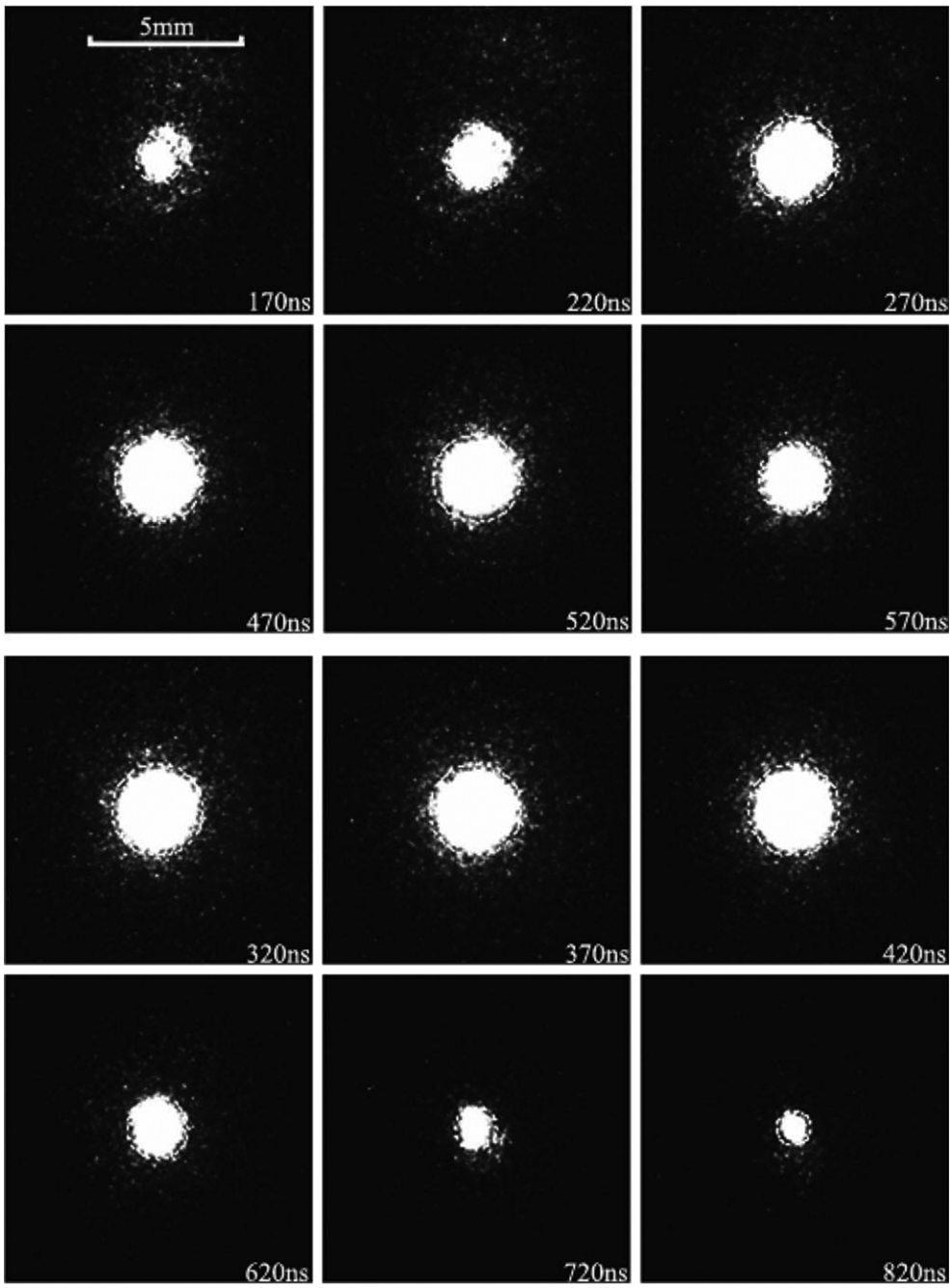

Figure 13. High-speed photographs of the plasma bullet in the surrounding air taken at head on with respect to the plasma plume. The exposure time is 5 ns. The internal diameter of the nozzle is 2.5 mm. Working gas is He/N_2 (He: 1 l min^{-1}; N_2: 0.015 l min^{-1}) mixture [117].

Naidis calculated the dependence of streamer propagation velocity on time for both polarities [51]. The simulation results show that the character of the calculated velocity with time agree with experiments reported by Jiang *et al* and Xiong *et al*. The velocities of positive and negative streamers, being nearly equal initially, vary with time quite differently. While at positive polarity the velocity changes rather slowly with time, at negative polarity a steep decrease with time takes place. As a result, the propagation length for the positive streamer is much larger than that for the negative one, which is also in agreement with reported experimental data.

4. Modes of operation of plasma jets under variable pressures

Recently Laroussi and Akman [108] studied the behavior of plasma plumes when the pressure of the environment in which they propagate changes. In their experiments, the plume/jet was injected into a chamber where the background pressure could be controlled. By lowering the pressure, less air molecules interact with the helium flow and a longer helium channel could be achieved. However, Laroussi and Akman discovered that the behavior of the plume was much more complicated as the pressure changed. They found that from atmospheric pressure to about 200 Torr, the plume increased

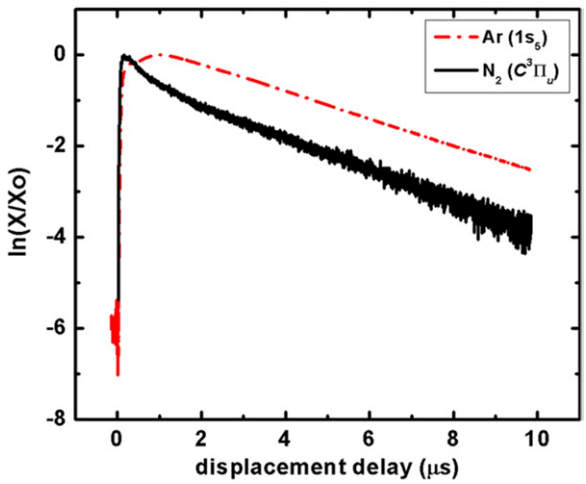

Figure 14. Decay of the Ar ($1s_5$) metastable line-integrated column density and N_2 ($C\ ^3\Pi_u$) emission intensity at 337 nm in the residual streamer channel 1 mm from the capillary tip [120].

in length relatively slightly. Below a pressure of 200 Torr and down to 70 Torr, a rapid increase in the length of the plasma plume was observed. However, below 70 Torr, the length of the plume started decreasing rather quickly while at the same time the plasma expanded in all directions, starting at the tip of the acrylic tube inside the chamber. Figure 16, which shows photographs of the plasma plume/jet inside the chamber at three different pressures, 760 Torr, 180 Torr and 75 Torr, illustrates the dramatic increase in the plume length for pressures below 200 Torr but above 70 Torr. The plasma plume/jet length reaches up to 25 cm at a pressure of 75 Torr. This is due to the fact that the ratio of helium mole fraction to that of air stays above the quenching threshold for longer distances.

When the pressure is below 70 Torr the plume length decreases while the plasma starts expanding in all directions. Figure 17, an image taken at a pressure of 18 Torr, clearly shows a shorter plume (as compared with the 75 Torr case) while a diffuse plasma expands from the tip of the acrylic tube.

It should be mentioned that this behavior is in agreement with calculations recently presented by Boeuf and Pitchford [107] who demonstrated that, for a helium jet propagating in air or nitrogen, the propagation is mainly associated with confinement of the ionization wave in the helium channel, where the ionization frequency is greater than in the surrounding gas. As a result, there is no radial expansion of the plasma. This also agrees with the simulation results reported by Naidis [115]. On the other hand, in pure helium, the ionization wave also moved radially, pushing the plasma toward the external part of the dielectric tube, thus inhibiting the on-axis propagation. Fewer air molecules interact with the helium flow and a longer helium channel could be achieved. As a result, the propagation distance should increase. But for a very low air/helium ratio, radial expansion of the plasma should occur, inducing a dramatic decrease in the confinement effect and consequently in the length of propagation. Breden *et al* showed that if a He discharge exists in pure He, there is no plasma bullet [71], which agrees with experimental results.

5. Interaction between plasma jets

As previously discussed, at atmospheric pressure the plasma jets can propagate over rather long distances but their diameters are limited to a few millimeters. Thus, they are not so convenient for large-scale applications. Indeed one single plasma jet can be progressively moved over the surface to be treated, but such an operating mode is very time consuming. A more efficient solution is to organize several plasma jets in 1D or 2D arrays, operating simultaneously from only one power supply. This concept was validated by several groups [21, 81, 131, 147–154] using either RF or kHz pulse excitation. But in all these configurations, strong uncontrolled interactions between the different jets frequently occur and must be minimized through a ballasting technique to allow good stability of the devices. On the other hand, it could be of interest to produce an interaction between two, or more, low diameter plasma jets impacting onto the same location of the target to increase the deposited dose of plasma, or to finely tune the composition of the reactive species using different feeding gas mixtures in each jet. Thus, a better understanding of the interaction between plasma jets would be valuable, and specific experiments in which two plasma jets were counter-propagating have been recently reported [155–157]. Algwari *et al* [155] used a T-tube (figure 18(*a*)) fed with helium, in which DBD jets were produced in the opposite arms. ICCD imaging of the device shows that two counter-propagating jets were produced. 150 ns after their ignition they entered into the perpendicular tube where they propagated independently along the tube wall for 200 ns. It is still unclear whether there is no interaction between the two plasmas or whether they are repelling each other. Then, they progressively merged into a single large plasma bullet propagating for additional 500 ns with a progressively decreasing luminosity. Sarron *et al* [156] used the device schematized in figure 18(*b*), which basically consisted of a circular ring inserted between two sections of a straight glass tube. The device was continuously flushed with pure neon. The spatio-temporal evolution of the plasma jet was analyzed with an ICCD camera with 15 ns exposure time. Time-resolved pictures showed that, at the entrance of the ring, the initial plasma bullet split into two bullets propagating symmetrically inside each branch of the ring, with a progressive decrease in velocity and luminous intensity. When they reached the straight exit section these two bullets merged into one, which then exhibited an intensity greater than that of the individual interacting bullets. Such behavior was interpreted as the evidence of a strong energy coupling through constructive ionization wave mixing. Kushner's group's simulation results showed good qualitative agreement with the experimental results [55, 56].

In the above-described experiments [155, 156], the interaction between the two counter-propagating plasma bullets was studied in structures continuously flushed with pure rare gas without turbulence and mixing between the rare gases and the ambient air. Indeed, such configurations are very convenient for fundamental studies; however, this is far from the actual situation encountered when several plasma jets should impact on a target located in free air. The interaction

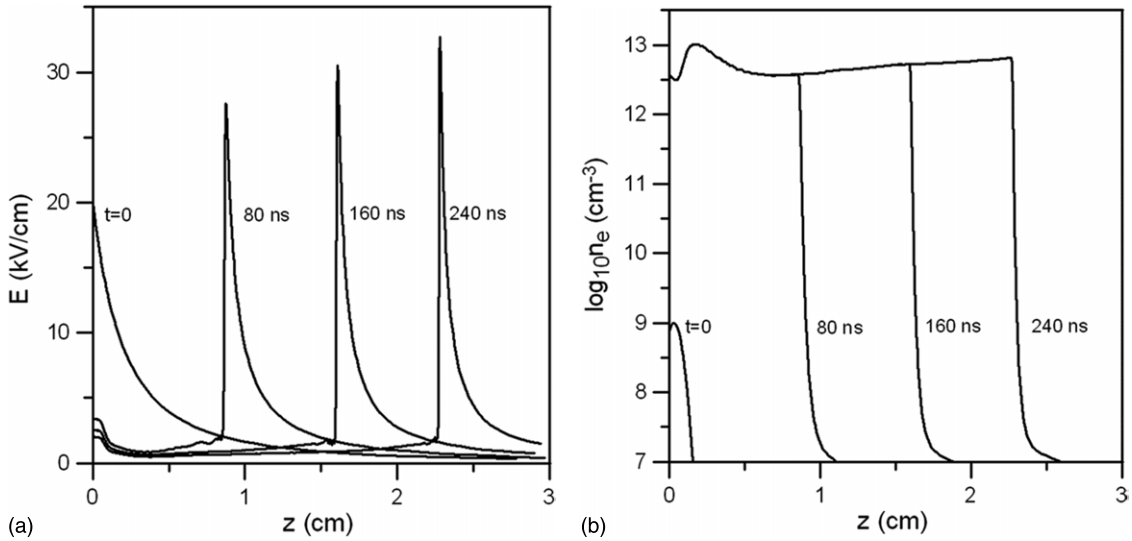

Figure 15. Profiles of electric field and number density of electrons along the symmetry axis at various times. The jet radius is 0.25 cm [121].

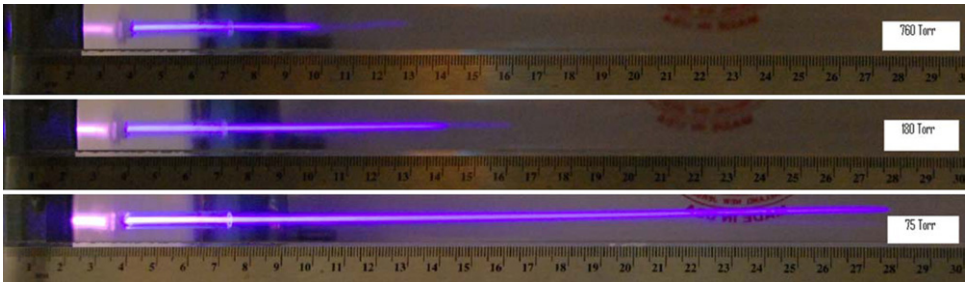

Figure 16. Photographs of the plasma jets at three different pressures showing a dramatic increase in plume length (as long the pressure stays higher than 70 Torr) [108].

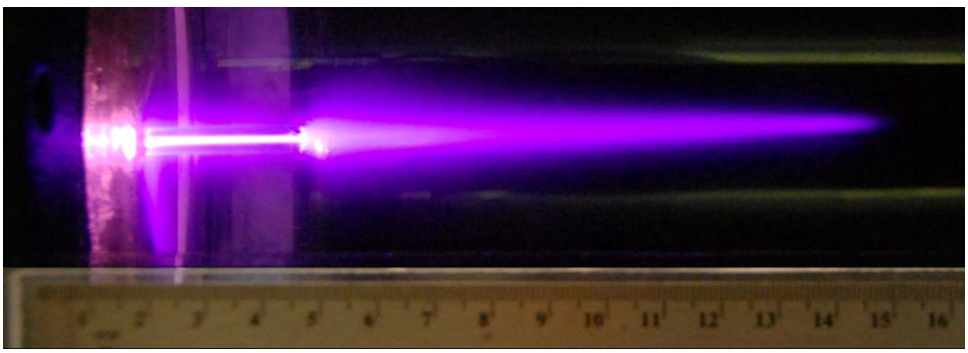

Figure 17. Photograph showing a shorter plume at a pressure of 18 Torr and showing plasma expansion at the base of the plume [108].

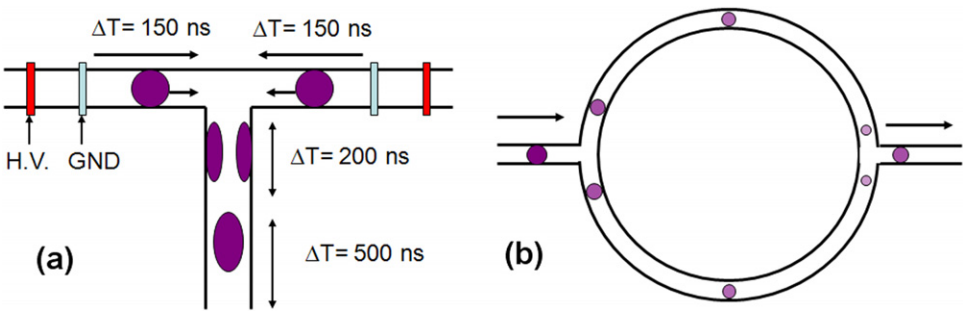

Figure 18. Schematic of the set-up used by Algwari *et al* [155] and by Sarron *et al* [156] to study the interaction of counter-propagating plasma bullets in a controlled atmosphere.

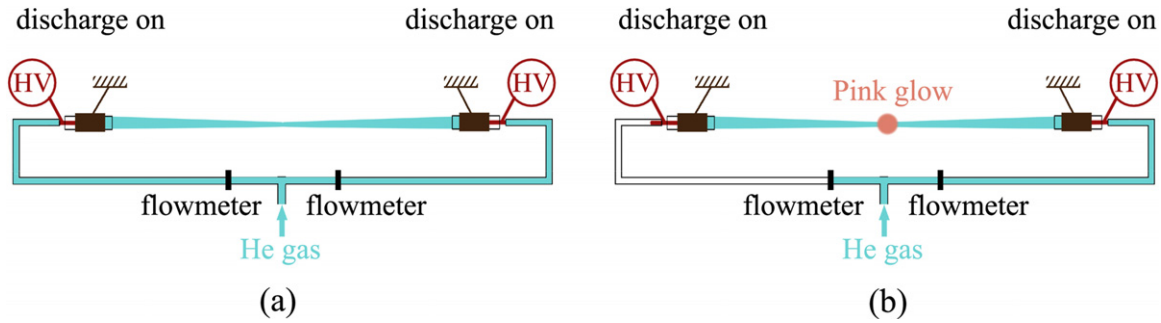

Figure 19. Schematic of the set-up used by Douat *et al* [157] to study the interaction of counter-propagating plasma bullets in ambient air. In (*a*) the helium gas flow is coming from two opposite directions, while in (*b*), helium is only fed inside the right device.

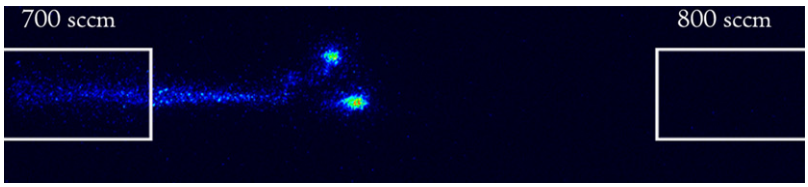

Figure 20. Branching occurring on a plasma jet propagating from left toward right when the right discharge was switched off. Pseudo-color picture taken with an exposure time of 5 ns. White rectangles correspond to the location of the DBD discharges.

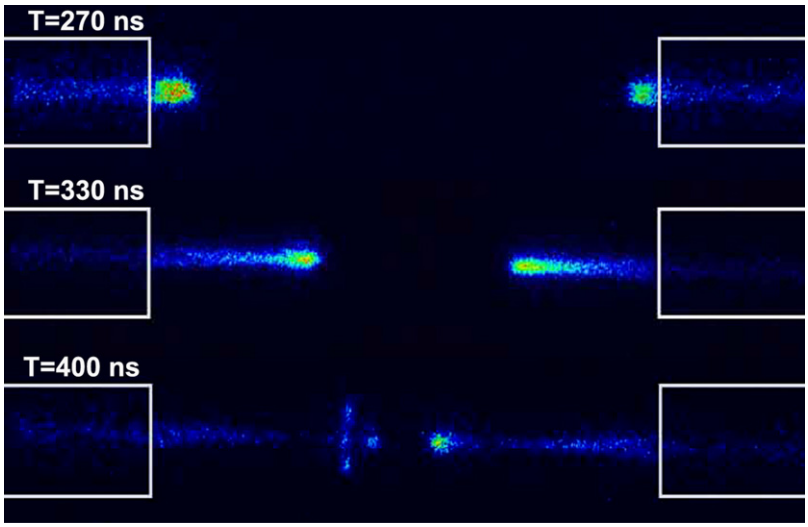

Figure 21. Time-resolved pictures (pseudo-colors, exposure time 5 ns) of the interaction between two plasma bullets counter-propagating in background air when helium is fed in each device.

between plasma jets counter-propagating in air was studied by Douat *et al* with the experimental set-up illustrated in figure 19.

The set-up mainly consisted of two coaxial dielectric barrier plasma jets facing each other at a distance of a few centimeters. HV pulses were applied between the electrodes at a repetition rate frequency of 20 kHz. The spatio-temporal evolution of the plasma emissions was investigated by an ICCD camera with exposure times of 5 ns. In the first set of experiments, corresponding to figure 19(*a*), helium was flowing through the two devices. When only the left discharge was switched on, time-resolved pictures clearly pointed out that, in the region of the helium/air/helium mixing, branching occurred in the plasma jet, with ramifications randomly propagating in radial directions, as shown in figure 20.

When the right discharge was also switched on, two counter-propagating plasma jets were produced. As far as they propagated against each other, the two plasma bullets interacted and their relative velocity decreased. When the distance between the two bullets became of the order of one millimeter, a 'secondary bullet' emerged, leaving behind a highly radial symmetrical luminous area, as shown in figure 21. This behavior was analyzed by Douat *et al* [157] as the signature of the radial expansion of an ion-dominated plasma.

In order to clarify these processes, a second set of experiments was performed with only one gas flow propagating from the right device toward the left one (figure 19(*b*)). For that condition, when the HV was only applied to the right device, the plasma jet easily reached the left device and penetrated inside its dielectric tube. But when the HV was also applied on the left device, a dramatic change occurred in the plasma evolution. Time-resolved studies of the plasma emission, figure 22, pointed out that up to the time $T = 380$ ns,

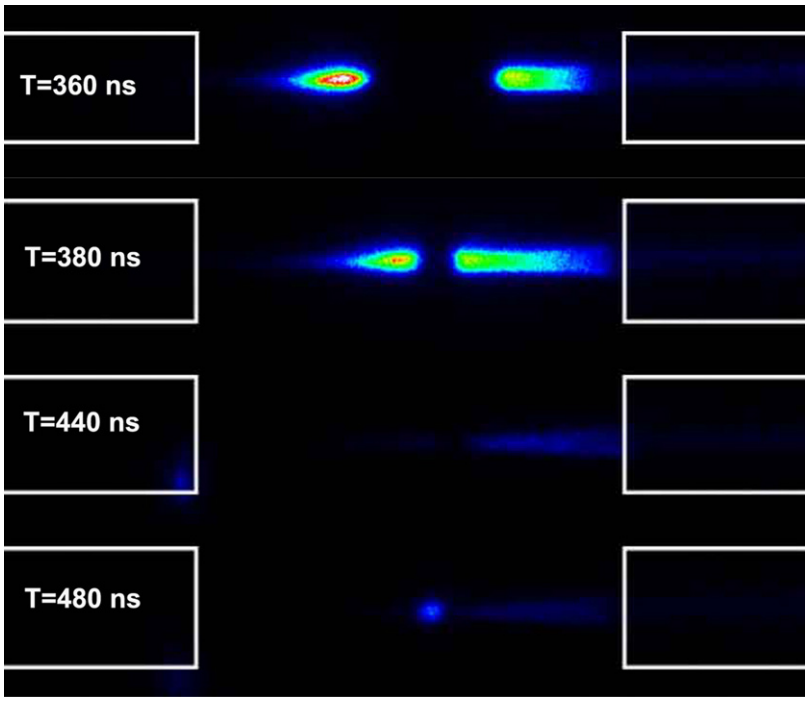

Figure 22. Time-resolved (exposure time 5 ns) pictures of the propagation of two counter-propagating plasma bullets with helium flowing from the right device toward the left one. Pictures are in pseudo-colors. In real ones, the spherical glow appearing at 480 ns in the mid-plan between the two DBDs is actually pink.

the two bullets counter-propagated similarly to the situation observed when the gas flows were coming from opposite directions. At $T = 380$ ns, the two plasma bullets were at their closest approach distance, leaving between them a space of about 0.8 mm free of luminous emission. From 380 to 450 ns, the emission intensity of each of the two counter-propagating plasmas decreased and finally vanished. But at $T = 460$ ns, a spherical pink glow suddenly appeared in the mid-plan between the two discharge devices, accurately positioned in the region which was previously free of plasma emission. After its ignition, the luminous intensity of this glow sharply increased, and in less than 30 ns, its magnitude was multiplied by a factor of 30. Afterwards, its emission intensity decreased and completely vanished in about 200 ns. Spectroscopic investigations demonstrated that this pink glow was associated with a large increase in the emission intensity of the first and second positive system of excited nitrogen, correlated with a decrease in the emission intensity of all the helium excited states, and of the nitrogen ions (first negative system at 391.4 nm) and excited oxygen atoms (transition at 777 nm), which are directly produced by energy transfer from the helium metastable states in non-equilibrium plasmas at atmospheric pressure. A more thorough discussion of the physical processes associated with the appearance of this pink glow is beyond the scope of the present review.

6. Summary

After about a decade of development, great progress has been made in understanding the operation of APNP-Js. Not only have various types of noble gas APNP-Js been reported, but also APNP-Js using N_2 and air have been introduced. In addition, the behavior of one of the most interesting phenomena of APNP-Js, the 'plasma bullet', has been much better understood. Some characteristics of traditional streamers and 'plasma bullet' are compared, such as the stochastic nature of their initiation, the ring-shaped profiles of plasma bullet radiation, the role of the dark channel left by the propagation of the plasma plume, and so on. However, there are still some features that are not well understood. For example, it is not clear whether an air/N_2 plasma plume has a similar dynamic behavior or not.

Further studies are now needed to enhance the chemical activity of the APNP-Js, so that the treatment time can be further shortened. In addition, development of APNP-Js with air as the working gas is still urgently needed since it will make many potential applications possible. Finally, for some applications, such as surface treatment, a large-area treatment is needed. How to make APNP-Js suitable for such applications is a topic of ongoing and future research effort.

Acknowledgments

The work of Lu is partially supported by the National Natural Science Foundation (Grant Nos 10875048 and 51077063), the Research Fund for the Doctoral Program of Higher Education of China (20100142110005) and the Chang Jiang Scholars Program, Ministry of Education, People's Republic of China. The work of Laroussi is supported by the US Air Force of Scientific Research. The work of Puech is supported by the French 'Agence Nationale de la Recherche' (program ANR 2010 BLAN 0930 01).

References

[1] Raizer Y P 1991 *Gas Discharge Physics* (Berlin: Springer)
[2] Lieberman M A 1994 *Principles of Plasma Discharges and Materials Processing* (New York: Wiley)
[3] Fridman A and Kennedy L A 2004 *Plasma Physics and Engineering* (New York: Taylor and Francis)
[4] Becker K H, Kogelschatz U, Schoenbach K H and Barker R J 2005 *Non-Equilibrium Air Plasmas at Atmospheric Pressure* (Bristol: Institute of Physics Publishing)
[5] Kogelschatz U 1990 *Pure Appl. Chem.* **62** 1667
[6] Chirokov A, Gutsol A, Fridman A, Dieber K D, Grace J M and Robinson K S 2004 *Plasma Sources Sci. Technol.* **13** 623
[7] Okazaki S, Kogoma M, Uehara M and Kimura Y 1993 *J. Phys. D: Appl. Phys.* **26** 889
[8] Shin J and Raja L 2006 *Appl. Phys. Lett.* **88** 021502
[9] Nersisyan G and Graham W G 2004 *Plasma Sources Sci. Technol.* **13** 582
[10] Laroussi M, Lu X, kolobov V and Arslanbekov R 2004 *J. Appl. Phys.* **96** 3028
[11] Xu P and Kushner M J 1998 *J. Appl. Phys.* **84** 4153
[12] Stollenwerk L, Amiranashvili S, Boeuf J P and Purwins H G 2006 *Phys. Rev. Lett.* **96** 255001
[13] Massines F and Gouda 1998 *J. Phys. D: Appl. Phys.* **31** 3411
[14] Babayan S E, Jeong J Y, Tu V J, Park J, Selwyn G S and Hicks R F 1998 *Plasma Sources Sci. Technol.* **7** 286
[15] Jeong J Y, Babayan S E, Tu V J, Park J, Henins I, Hicks R F and Selwyn G S 1998 *Plasma Source Sci. Technol.* **7** 282
[16] Jeong J Y, Babayan S E, Schutz A, Tu V J, Park J, Henins I, Selwyn G S and Hicks R F 1999 *J. Vac. Sci. Technol.* A **17** 2581
[17] Park J, Henins I, Herrmann H W, Selwyn G S, Jeong J Y, Hicks R F, Shim D and Chang C S 2000 *Appl. Phys. Lett.* **76** 288
[18] Babayan S E, Jeong J Y, Schutze A, Tu V J, Moravej M, Selwyn G S and Hicks R F 2001 *Plasma Sources Sci. Technol.* **10** 573
[19] Moravej M, Yang X, Nowling G R, Chang J P, Hicks R F and Babayan S E 2004 *J. Appl. Phys.* **96** 7011
[20] Xu L, Liu P, Zhan R J, Wen X H, Ding L L and Nagatsu M 2006 *Thin Solid Films* **506–507** 400
[21] Hubicka Z, Cada M, Sicha M, Churpita A, Pokorny P, Soukup L and Jastrabik L 2002 *Plasma Sources Sci. Technol.* **11** 195
[22] Leveille V and Coulombe S 2005 *Plasma Sources Sci. Technol.* **14** 467
[23] Yonson S, Coulombe S, Leveille V and Leask R L 2006 *J. Phys. D: Appl. Phys.* **39** 3508
[24] Xiong Q, Nikiforov A, Lu X and Leys C 2010 *J. Phys. D: Appl. Phys.* **43** 415201
[25] Teschke M, Kedzierski J, Finantu-Dinu E G, Korzec D and Engemann J 2005 *IEEE Trans. Plasma Sci.* **33** 310
[26] Li Q, Li J T, Zhu W C, Zhu X M and Pu Y K 2009 *Appl. Phys. Lett.* **95** 141502
[27] Lu X, Jiang Z, Xiong Q, Tang Z, Hu X and Pan Y 2008 *Appl. Phys. Lett.* **92** 081502
[28] Walsh J L and Kong M G 2008 *Appl. Phys. Lett.* **93** 111501
[29] Lu X, Jiang Z, Xiong Q, Tang Z and Pan Y 2008 *Appl. Phys. Lett.* **92** 151504
[30] Laroussi M and Lu X 2005 *Appl. Phys. Lett.* **87** 113902
[31] Shashurin A, Shneider M N, Dogariu A, Miles R B and Keidar M 2009 *Appl. Phys. Lett.* **94** 231504
[32] Stoffels E, Kieft I E and Sladek R E J 2003 *J. Phys. D: Appl. Phys.* **36** 2908
[33] Lu X *et al* 2009 *IEEE Trans. Plasma Sci.* **37** 668
[34] Hong Y C and Uhm H S 2006 *Appl. Phys. Lett.* **89** 221504
[35] Ni T L, Ding F, Zhu X D, Wen X H and Zhou H Y 2008 *Appl. Phys. Lett.* **92** 241503
[36] Hong Y C, Uhm H S and Yi W J 2008 *Appl. Phys. Lett.* **93** 051504
[37] Hong Y C and Uhm H S 2007 *Phys. Plasmas* **14** 053503
[38] Mohamed A H, Kolb J F and Schoenbach K H 2009 *US Patent* 7,572,998 B2
[39] Hong Y, Kang W, Hong Y, Yi W and Uhm H 2009 *Phys. Plasmas* **16** 123502
[40] Fridman G 2006 *Plasma Chem. Plasma Process.* **26** 425
[41] Wu S, Lu X, Xiong Z and Pan Y 2010 *IEEE Trans. Plasma Sci.* **38** 3404
[42] Machala Z, Laux C and Kruger C 2005 *IEEE Trans. Plasma Sci.* **33** 320
[43] Lu X, Xiong Z, Zhao F, Xian Y, Xiong Q, Gong W, Zou C, Jiang Z and Pan Y 2009 *Appl. Phys. Lett.* **95** 181501
[44] Forster S, Mohr C and Viol W 2005 *Surf. Coat. Technol.* **200** 827
[45] Schneider S, Lackmann J W, Narberhaus F, Bandow J E, Denis B and Benedikt J 2011 *J. Phys. D: Appl. Phys.* **44** 295201
[46] Qian M, Ren C, Wang D, Zhang J and Wei G 2010 *J. Appl. Phys.* **107** 063303
[47] Porteanu H E, Kühn S and Gesche R 2010 *J. Appl. Phys.* **108** 013301
[48] Yuji T, Kawano H, Kanazawa S, Ohkubo T and Akatsuka H 2008 *IEEE Trans. Plasma Sci.* **36** 976
[49] Tsai T-C and Staack D 2011 *Plasma Process. Polym.* **8** 523
[50] Sousa J S, Niemi K, Cox L J, Algwari Q T, Gans T and O'Connell D 2011 *J. Appl. Phys.* **109** 123302
[51] Naidis G 2011 *Appl. Phys. Lett.* **98** 141501
[52] Reuter S, Niemi K, Schulz-von der Gathen V and Dobele H F 2009 *Plasma Sources Sci. Technol.* **18** 015006
[53] Fricke K, Steffen H, von Woedtke T, Schröder K and Weltmann K-D 2011 *Plasma Process. Polym.* **8** 51
[54] Oh J S, Olabanji O T, Hale C, Mariani R, Kontis K and Bradley J W 2011 *J. Phys. D: Appl. Phys.* **44** 155206
[55] Xiong Z, Takashiman K, Adamovich I and Kushner M 2011 Simulation of high pressure ionization waves in straight and circuitous dielectric channels *64th Gaseous Electronics Conf. (Salt Lake City, UT, 14–18 November 2011)*
[56] Kushner M 2011 Interaction of high pressure plasmas with their boundaries: channels, tubes, liquids and tissue *30th Int. Conf. on Phenomena in Ionized Gases (Belfast, UK, 28 August–2 September 2011)*
[57] Cho G, Lim H, Kim J H, Jin D J, Kwon G C, Choi E H and Uhm H S 2011 *IEEE Trans. Plasma Sci.* **39** 1234
[58] Dgheim J 2007 *Plasma Sources Sci. Technol.* **16** 211
[59] Kim H, Brockhaus A and Engemann J 2009 *Appl. Phys. Lett.* **95** 211501
[60] Laimer J, Reicher H and Stori H 2009 *Vacuum* **84** 104
[61] Schafer J, Sigeneger F, Foest R, Loffhagen D and Weltmann K D 2010 *Eur. Phys. J.* D **60** 531
[62] Georgescu N, Lungu C P, Lupu A R and Osiac M 2010 *IEEE Trans. Plasma Sci.* **38** 3156
[63] Bibinov N, Dudek D, Awakowicz P and Engemann J 2007 *J. Phys. D: Appl. Phys.* **40** 7372
[64] Pipa A V and Ropcke J 2009 *IEEE Trans. Plasma Sci.* **37** 1000
[65] Knake N, Reuter S, Niemi K, Schulz-von der Gathen V and Winter J 2008 *J. Phys. D: Appl. Phys.* **41** 194006
[66] Knake N, Niemi K, Reuter S, Schulz-von der Gathen V and Winter J 2008 *Appl. Phys. Lett.* **93** 131503
[67] Pipa A V, Bindemann T, Foest R, Kindel E, Ropcke J and Weltmann K D 2008 *J. Phys. D: Appl. Phys.* **41** 194011
[68] Hong Y, Yoo S and Lee B 2011 *J. Electrostat.* **69** 92
[69] Nie Q Y, Ren C S, Wang D Z, Li S Z, Zhang J L and Kong M G 2007 *Appl. Phys. Lett.* **90** 221504
[70] Li Q, Takana H, Pu Y K and Nishiyama H 2011 *Appl. Phys. Lett.* **98** 241501
[71] Breden D, Miki K and Raja L L 2011 *Appl. Phys. Lett.* **99** 111501

[72] Lim J P, Uhm H S and Li S Z 2007 *Appl. Phys. Lett.* **90** 051504
[73] Laroussi M and Akan T 2007 *Plasma Process. Polym.* **4** 777
[74] Iza F, Kim G J, Lee S M, Lee J K, Walsh J L, Zhang Y T and Kong M 2008 *Plasma Process. Polym.* **5** 322
[75] Jansky J and Bourdon A 2011 *Appl. Phys. Lett.* **99** 161504
[76] Algwari T and O'Connell D 2011 *Appl. Phys. Lett.* **99** 121501
[77] Xiong Z *et al* 2010 *IEEE Trans. Plasma Sci.* **38** 1001
[78] Xiong Q *et al* 2009 *J. Appl. Phys.* **106** 083302
[79] Stonies R, Schermer S, Voges E and Broekaert J A C 2004 *Plasma Sources Sci. Technol.* **13** 604
[80] Xiong Q, Lu X, Jiang Z, Tang Z, Hu J, Xiong Z, Hu X and Pan Y 2008 *IEEE Trans. Plasma Sci.* **36** 986
[81] Lu X, Xiong Q, Tang Z, Jiang Z and Pan Y 2008 *IEEE Trans. Plasma Sci.* **36** 990
[82] Yan J D, Pau C F, Wylie S R and Fang M T C 2002 *J. Phys. D: Appl. Phys.* **35** 2594
[83] Kuo S P, Tarasenko O, Popovic S and Levon K 2006 *IEEE Trans. Plasma Sci.* **34** 1275
[84] Laroussi M 2005 *Plasma Process. Polym.* **2** 391
[85] Laroussi M 2009 *IEEE Trans. Plasma Sci.* **37** 714
[86] Kong M, Kroesen G, Morfill G, Nosenko T, Shimizu T, Dijk J and Zimmermann J 2009 *New J. Phys.* **11** 115012
[87] Perni S, Deng X, Shama G and Kong M 2006 *IEEE Trans. Plasma Sci.* **34** 1297
[88] Morfill G E, Kong M and Zimmermann J L 2009 *New J. Phys.* **11** 115011
[89] Fridman G, Friedman G, Gutsol A, Shekhter A B, Vasilets V N and Fridman A 2008 *Plasma Process. Polym.* **5** 503
[90] Fridman G, Brooks A, Galasubramanian M, Fridman A, Gutsol A, Vasilets V, Ayan H and Friedman G 2007 *Plasma Process. Polym.* **4** 370
[91] Shashurin A, Keidar M, Bronnikov S, Jurjus R A and Stepp M A 2008 *Appl. Phys. Lett.* **93** 181501
[92] Mariotti D 2008 *Appl. Phys. Lett.* **92** 151505
[93] Kim G C, Kim G J, Park S R, Jeon S M, Seo H J, Iza F and Lee J K 2009 *J. Phys. D: Appl. Phys.* **42** 032005
[94] Dobrynin D, Fridman G and Friedman G 2009 *New J. Phys.* **11** 115020
[95] Sladek R E J, Stoffels E, Walraven R, Tielbeek P J A and Koolhoven R A 2004 *IEEE Trans. Plasma Sci.* **32** 1540
[96] O'Connell D, Cox L J, Hyland W B, McMahon S J, Reuter S, Graham W G, Gans T and Currell F J 2011 *Appl. Phys. Lett.* **98** 043701
[97] Yang S S, Kim K, Choi J D, Hong Y C, Kim G, Noh E J and Lee J S 2011 *Appl. Phys. Lett.* **98** 073701
[98] Abramzon N, Joaquin J C, Bray J and Brelles-Marino G 2006 *IEEE Trans. Plasma Sci.* **34** 1304
[99] Daeschlein G, Scholz S, von Woedtke T, Niggemeier M, Kindel E, Brandenburg R, Weltmann K D and Junger M 2011 *IEEE Trans. Plasma Sci.* **39** 815
[100] Chung T H, Kim S J, Bae S H and Leem S H 2009 *Appl. Phys. Lett.* **94** 141502
[101] Xiong Z, Lu X, Feng A, Pan Y and Ostrikov K 2010 *Phys. Plasmas* **17** 123502
[102] Yan X *et al* 2010 *IEEE Trans. Plasma Sci.* **38** 2451
[103] Zhou X, Xiong Z, Cao Y, Lu X and Liu D 2010 *IEEE Trans. Plasma Sci.* **38** 3370
[104] Yan X *et al* 2009 *Appl. Phys. Lett.* **95** 083702
[105] Lu X, Ye T, Cao Y, Sun Z, Xiong Q, Tang Z, Xiong Z, Hu J, Jiang Z and Pan Y 2008 *J. Appl. Phys.* **104** 053309
[106] Xiong Z, Du T, Lu X, Cao Y and Pan Y 2011 *Appl. Phys. Lett.* **98** 221503
[107] Boeuf J P and Pitchford L C 2011 *6th Int. Conf. on Microplasmas (Paris, France, 3–6 April 2011)*
[108] Laroussi M and Akman M A 2011 *AIP Adv.* **1** 032138
[109] Lu X and Laroussi M M 2006 *J. Appl. Phys.* **100** 063302
[110] Dawson G A and Winn W P 1965 *Z. Phys.* **183** 159
[111] Xian Y, Lu X, Cao Y, Yang P, Xiong Q, Jiang Z and Pan Y 2009 *IEEE Trans. Plasma Sci.* **37** 2068
[112] Walsh J L, Iza F, Janson N B, Law V J and Kong M G 2010 *J. Phys. D: Appl. Phys.* **43** 075201
[113] Mericam-Bourdet N, Laroussi M, Begum A and Karakas E 2009 *J. Phys. D: Appl. Phys.* **42** 055207
[114] Sakiyama Y, Graves D, Jarrige J and Laroussi M 2010 *Appl. Phys. Lett.* **96** 041501
[115] Naidis G V 2011 *J. Phys. D: Appl. Phys.* **44** 215203
[116] Zhu W, Li Q, Zhu X and Pu Y 2009 *J. Phys. D: Appl. Phys.* **42** 202002
[117] Wu S, Huang Q, Wang Z and Lu X 2011 *IEEE Trans. Plasma Sci.* **PP** 2123912
[118] Lu X, Jiang Z, Xiong Q, Tang Z, Xiong Z, Hu J, Hu X and Pan Y 2008 *IEEE Trans. Plasma Sci.* **36** 988
[119] Karakas E and Laroussi M 2010 *J. Appl. Phys.* **108** 063305
[120] Sands B, Leiweke R J and Ganguly B 2010 *J. Phys. D: Appl. Phys.* **43** 282001
[121] Naidis G V 2010 *J. Phys. D: Appl. Phys.* **43** 402001
[122] Jiang C, Chen M T and Gundersen M A 2009 *J. Phys. D: Appl. Phys.* **42** 232002
[123] Xiong Z, Lu X, Xian Y, Jiang Z and Pan Y 2010 *J. Appl. Phys.* **108** 103303
[124] Ohyama R, Sakamoto M and Nagai A 2009 *J. Phys. D: Appl. Phys.* **42** 105203
[125] Jiang N, Ji A and Cao Z 2009 *J. Appl. Phys.* **106** 013308
[126] Jiang N, Ji A and Cao Z 2010 *J. Appl. Phys.* **108** 033302
[127] Walsh J L, Shi J J and Kong M G 2006 *Appl. Phys. Lett.* **88** 171501
[128] Walsh J L and Kong M G 2008 *IEEE Trans. Plasma Sci.* **36** 954
[129] Walsh J L and Kong M G 2007 *Appl. Phys. Lett.* **91** 221502
[130] Nie Q Y, Cao Z, Ren C S, Wang D Z and Kong M G 2009 *New J. Phys.* **11** 115015
[131] Cao Z, Nie Q, Bayliss D L, Walsh J L, Ren C S, Wang D Z and Kong M G 2010 *Plasma Sources Sci. Technol.* **19** 025003
[132] Cao Z, Nie Q Y and Kong M G 2009 *J. Phys. D: Appl. Phys.* **42** 222003
[133] Kong M G, Nie Q Y, Cao Z, Ren C S and Wang D Z 2009 *New J. Phys.* **11** 115015
[134] Shi J J, Liu D W and Kong M G 2007 *IEEE Trans. Plasma Sci.* **35** 137
[135] Sands B L, Ganguly B N and Tachibana K 2008 *IEEE Trans. Plasma Sci.* **36** 956
[136] Sands B L, Ganguly B N and Tachibana K 2008 *Appl. Phys. Lett.* **92** 151503
[137] Urabe K, Ito Y, Tachibana K and Ganguly B N 2008 *Appl. Phys. Express* **1** 066004
[138] Urabe K, Morita T, Tachibana K and Ganguly B N 2010 *J. Phys. D: Appl. Phys.* **43** 095201
[139] Laroussi M, Tendero C, Lu X, Alla S and Hynes W L 2006 *Plasma Process. Polym.* **3** 470
[140] Laroussi M, Hynes W, Akan T, Lu X and Tendero C 2008 *IEEE Trans. Plasma Sci.* **36** 1298
[141] Chung T H, Kim S J and Bae S H 2010 *Phys. Plasmas* **17** 053504
[142] Chen L W, Zhao P, Shu X S, Shen J and Meng Y D 2010 *Phys. Plasmas* **17** 083502
[143] Xiong Q *et al* 2010 *J. Appl. Phys.* **107** 073302
[144] Xian Y, Lu X, Tang Z, Xiong Q, Gong W, Liu D, Jiang Z and Pan Y 2010 *J. Appl. Phys.* **107** 063308
[145] Lu X *et al* 2009 *J. Appl. Phys.* **105** 043304
[146] Lu X, Xiong Q, Xiong Z, Hu J, Zhou F, Gong W, Xian Y Zhou C, Tang Z, Jiang Z and Pan Y 2009 *Thin Solid Films* **518** 967
[147] Koretzky E and Kuo S P 1998 *Phys. Plasmas* **5** 3774
[148] Kuo S P, Koretzky E and Orlick L 1999 *IEEE Trans. Plasma Sci.* **27** 752
[149] Foest R, Kindel E, Ohl A, Stieber M and Weltmann K D 2005 *Plasma Phys. Control. Fusion* **47** B525

[150] Chichina M, Hubicka Z, Churpita O and Tichy M 2005 *Plasmas Process. Polym.* **2** 501
[151] Hong Y C, Shin D H, Lee S C and Uhm H S 2006 *Thin Solid Films* **506–507** 474
[152] Hong Y C, Cho S C and Uhm H S 2007 *Appl. Phys. Lett.* **90** 141501
[153] Tang D, Ren C, Wang D and Nie Q 2009 *Plasma Sci. Technol.* **11** 293
[154] Cao Z, Walsh J L and Kong M G 2009 *Appl. Phys. Lett.* **94** 021501
[155] Algwari Q Th, Neill C O and O'Connell D 2009 *62nd Gaseous Electronics Conf. (Saratoga Springs, NY)* p 69
[156] Sarron V, Robert E, Doziat S, Vandamme M, Ries D and Pouvesle J M 2011 *IEEE Trans. Plasma Sci.* **39** 2856
[157] Douat C, Fleury M, Laroussi M and Puech V 2011 *IEEE Trans. Plasma Sci.* **39** 2298